



Integrated Network Pharmacology Analysis and Experimental Validation to Investigate the Mechanism of Zhi-Zi-Hou-Po Decoction in Depression

Yongtao Bai^{1,2†}, Yingchun Zhang^{3†}, Shuolei Li², Wenzhou Zhang¹, Xinhui Wang³, Baoxia He^{1,2*} and Wenzheng Ju^{4*}

OPEN ACCESS

Edited by:

Aiping Lu,
Hong Kong Baptist University, Hong Kong, SAR China

Reviewed by:

Kan He,
Anhui University, China
Clara Grosso,
LAQV Network of Chemistry and Technology, Portugal
Daogang Guan,
Southern Medical University, China

*Correspondence:

Baoxia He
hbxberry@sina.com
Wenzheng Ju
juwz333@hotmail.com

[†]These authors have contributed equally to this work and share first authorship

Specialty section:

This article was submitted to Ethnopharmacology, a section of the journal *Frontiers in Pharmacology*

Received: 18 May 2021

Accepted: 07 September 2021

Published: 08 October 2021

Citation:

Bai Y, Zhang Y, Li S, Zhang W, Wang X, He B and Ju W (2021) Integrated Network Pharmacology Analysis and Experimental Validation to Investigate the Mechanism of Zhi-Zi-Hou-Po Decoction in Depression. *Front. Pharmacol.* 12:711303. doi: 10.3389/fphar.2021.711303

¹Department of Pharmacy, Affiliated Cancer Hospital of Zhengzhou University, Henan Cancer Hospital, Zhengzhou, China, ²Phase I Clinical Research Center, Affiliated Cancer Hospital of Zhengzhou University, Henan Cancer Hospital, Zhengzhou, China, ³College of Pharmaceutical Sciences and Chinese Medicine, Southwest University, Chongqing, China, ⁴Department of Clinical Pharmacology, Affiliated Hospital of Nanjing University of Chinese Medicine, Nanjing, China

Zhi-Zi-Hou-Po Decoction (ZZHPD) is a well-known traditional Chinese medicine (TCM) that has been widely used in depression. However, the antidepressant mechanism of ZZHPD has not yet been fully elucidated. The purpose of this study was to explore the pharmacological mechanisms of ZZHPD acting on depression by combining ultra flow liquid chromatography with quadrupole time-of-flight mass spectrometry (UFLC-Q-TOF/MS) and network pharmacology strategy. The chemical components of ZZHPD were identified using UFLC-Q-TOF/MS, while the potential drug targets and depression-related targets were collected from databases on the basis of the identified compounds of ZZHPD. Protein-protein interaction (PPI) network, gene ontology (GO), and Kyoto encyclopedia of genes and genomes (KEGG) pathway enrichment analyses were used to unravel potential antidepressant mechanisms. The predicted antidepressant targets from the pharmacology-based analysis were further verified *in vivo*. As a result, a total of 31 chemical compounds were identified by UFLC-Q-TOF/MS; 514 promising drug targets were mined by using the Swiss Target Prediction; and 527 depression-related target genes were pinpointed by the GeneCards and OMIM databases. STRING database and Cytoscape's topological analysis revealed 80 potential targets related to the antidepressant mechanism of ZZHPD. The KEGG pathway analysis revealed that the antidepressant targets of ZZHPD were mainly involved in dopaminergic synapse, serotonin synapse, cAMP, and mTOR signaling pathways. Furthermore, based on the animal model of depression induced by chronic corticosterone, the regulatory effects of ZZHPD on the expression of MAOA, MAOB, DRD2, CREBBP, AKT1, MAPK1, HTR1A, and GRIN2B mRNA levels as well as the cAMP signaling pathway and monoaminergic metabolism were experimentally verified in rats. Our study revealed that ZZHPD is expounded to target various genes and pathways to perform its antidepressant effect.

Keywords: Zhi-Zi-Hou-Po decoction, UFLC-Q-TOF/MS, network pharmacology, depression, CAMP signaling pathway

INTRODUCTION

Depression, a prevalent mental illness with high economic and social costs, poses a major risk for human health (Shafiee et al., 2018; Wang et al., 2020). Major depressive disorder (MDD) shows the characteristics of “three highs,” that is, high prevalence, high recurrence rate, and high disability rate (GBD 2015 Disease and Injury Incidence and Prevalence Collaborators, 2016; Khosravi et al., 2020). From 1990 to 2017, the prevalence of depression in China increased from 3,224.6 per 100,000 to 39,905/100,000, with an increased rate of 24.7%. Among the cases, women and adults over 55 years of age are at a high risk of depression, which is a huge challenge to China’s healthcare (Ren et al., 2020). Although diverse hypotheses have been suggested, including monoaminergic deficiency, immune system disorders, hypothalamic-pituitary-adrenal axis (HPA) imbalance, neurotrophic factors reduction, and neuroplasticity pathway impairment, the exact neurobiological mechanism of depression is still unclear (Dean and Keshavan, 2017; Robson et al., 2017; Levy et al., 2018). In current clinical practice, most antidepressants primarily act by targeting the monoamine neurotransmitter system, such as fluoxetine or venlafaxine. However, these drugs often lead to obvious adverse effects, such as fractures, upper gastrointestinal bleeding, adverse drug reactions, and withdrawal symptoms (Coupland et al., 2018; Hengartner et al., 2019). Thus, it is necessary to find an alternative antidepressant with low toxicity and high efficiency.

As we know, TCM has been used in clinic for thousands of years in China and has played an important role in people’s health. At present, TCM is still an efficient and reliable resource for drug discovery (Cheung, 2011; Han et al., 2020). Many studies have shown that TCM has broad prospects in the prevention and treatment of major depression disorder (Sun et al., 2018; Ye et al., 2019). Zhi-Zi-Hou-Po Decoction (ZZHPD), being composed of the stem, branch, and root barks of *Magnolia officinalis* Rehder & E.H.Wilson (Hou-Po, HP), the ripe fruit of *Gardenia jasminoides* J.Ellis (Zhi-Zi, ZZ), and the young fruit of *Citrus × aurantium* L. (Zhi-Shi, ZS), is a classic prescription for relieving restlessness and removing fullness in the TCM masterpiece “Treatise on Febrile and Miscellaneous Diseases,” compiled by Zhang Zhongjing (AD 150–219) (Wang and Feng, 2019; Zhang and Feng, 2020). ZZHPD has often been utilized in clinical practice to treat mental disorders, especially major depression disorder (Luo and Feng, 2016). There is accumulating evidence that ZZHPD can significantly improve depressive symptoms by balancing energy metabolism, monoaminergic system, and amino acid metabolism and enhancing hippocampal neurogenesis (Xing et al., 2015; Xing et al., 2019). In addition, some studies have found that a single herb of ZZHPD had an antidepressant effect in animals. Two standardized fractions of Zhi-Zi had an antidepressant-like effect associated with BDNF signaling in mice (Ren et al., 2016; Ruan et al., 2019). Acute treatments with Hou-Po extract could attenuate the forced swim-induced experimental depression in mice (Nakazawa et al., 2003), and Zhi-Shi aqueous extract was proved to have an antidepressant effect *in vivo* and *in vitro* (Wu M. et al., 2015). Although the effects of ZZHPD and the single herb on depression have been

studied, the antidepressant mechanism has not yet been systematically clarified because of the complexity of ZZHPD with multiple compositions.

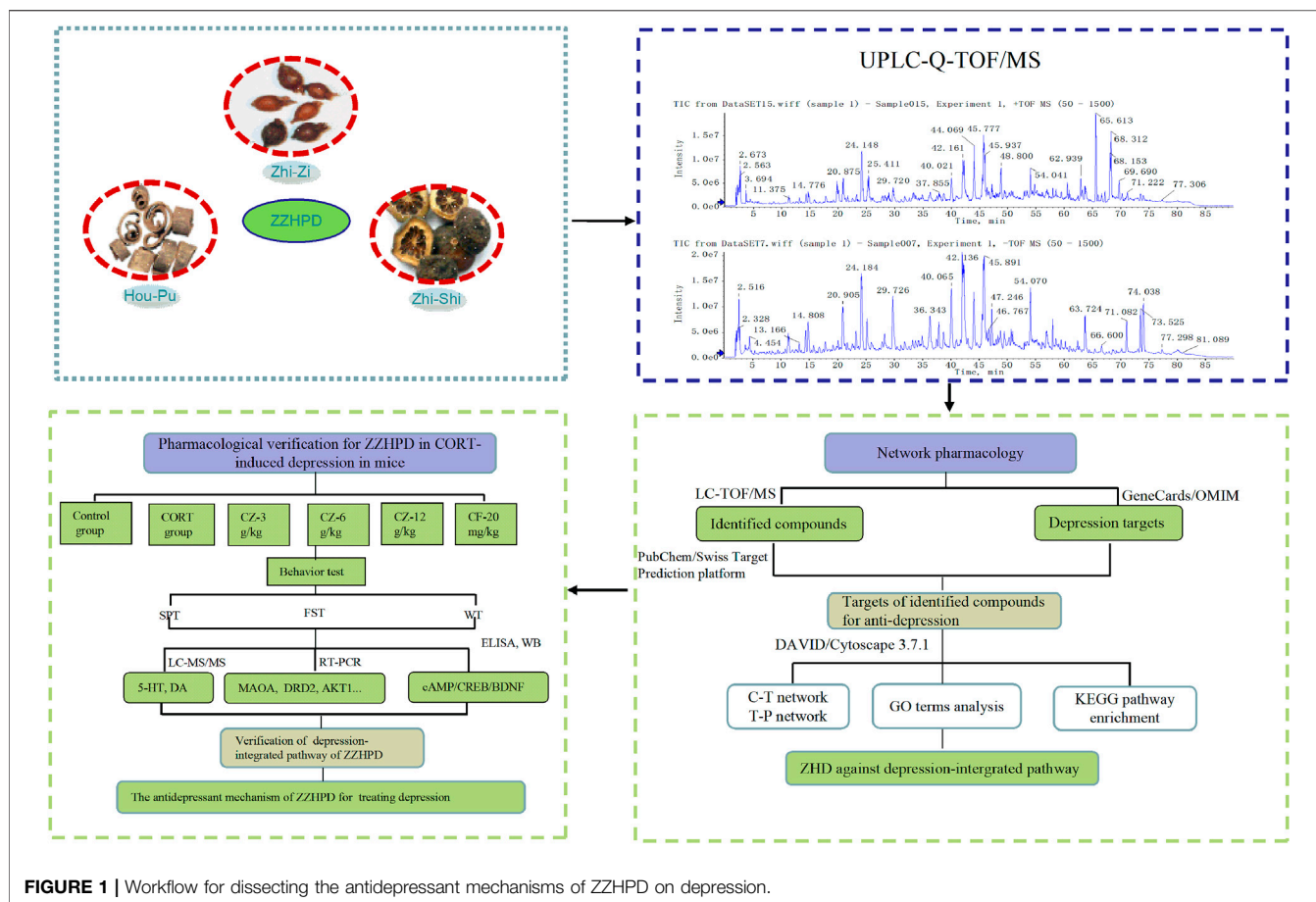
Network pharmacology is a comprehensive approach for modern TCM research that integrates multiple disciplines including bioinformatics, systems biology, and traditional pharmacology (Zhang R. et al., 2019). As a new methodology, network pharmacology conforms to the holistic view and the principle of syndrome differentiation and treatment system of TCM, thus providing different research thoughts and feasible technical approaches for probing into the underlying mechanism of Chinese herbal formulae (Banerjee et al., 2019; Yu et al., 2019).

In this context, firstly, we used the UFLC-Q-TOF/MS to identify the chemical composition of alcohol extracts of ZZHPD. Next, we mined the potential mechanisms in the treatment of depression using network pharmacology based on the identified phytochemical components of ZZHPD. Several databases were used to collect information in order to predict the phytochemical compound targets, depression-related molecular targets, molecular signaling, and network construction. Finally, a rat depression model induced by corticosterone injection was established to verify the predicted antidepressant targets from pharmacology-based analysis (Figure 1). This study showed that the antidepressant activity of ZZHPD involves the regulation of the expression of MAOA, MAOB, DRD2, CREBBP, AKT1, MAPK1, and HTR1A mRNA levels, as well as the monoaminergic system and cAMP signaling pathway. The present study was the first to use UFLC-Q-TOF/MS-based network pharmacology to explore the possible antidepressant mechanisms of ZZHPD, thereby improving the understanding of this representative antidepressant herbal prescription, which will help to extend its further practical application for patients with depression.

MATERIALS AND METHODS

Materials and Reagents

Reference substance synephrine, geniposide, naringin, neohesperidin, geniposidic acid, chlorogenic acid, caffeic acid, hesperidin, rutin, honokiol, magnolol, and deacetyl asperulosidic acid methyl ester (purity > 98% by HPLC, respectively) were obtained from Chengdu Munster Biotechnology Co., Ltd. (Chengdu, Sichuan, China). Genipin 1-gentiobioside (99.1% by HPLC) was supplied by Shanghai Yuanye Bio-Technology (Shanghai, China). Formic acid (MS-grade), dopamine (DA), and serotonin (5-HT) were from Sigma-Aldrich (St. Louis, MO, United States). The ripe fruit of *Gardenia jasminoides* J. Ellis was originally harvested in Hubei and the stem bark of *Magnolia officinalis* Rehder and E. H. Wilson and the young fruit of *Citrus × aurantium* L. were grown in Sichuan, and they were provided by Beijing Tongrentang Pharmacy (Beijing, China) with batch numbers 20150301, 20150301, and 150401, respectively, and were authenticated by Dr. Qian Zhang from the Jiangsu Province Hospital of Chinese Medicine (Nanjing, Jiangsu, China). Fluoxetine (Flu) was obtained from Lilly Co., Ltd. (Suzhou, Jiangsu, China). Corticosterone was supplied by



Tokyo Chemical Industry Co., Ltd. (Shanghai, China). Methanol, acetonitrile, and pyridine (MS-grade) were supplied by Merck Company (Darmstadt, Germany). The ultrapure water was produced by a Milli-Q purification instrument (Milford, MA, United States). And other reagents used in the experiment were of analytical grade and purchased from commercial reagent companies.

Standard Sample Preparation

Reference standards were precisely weighed using a Sartorius balance with 1/100,000 accuracy and diluted in methanol to prepare stock solutions except for hesperidin, which was dissolved in methanol-pyridine solution (50:50). Before use, these individual reference stock solutions were mixed according to an appropriate amount of each standard sample and then diluted in methanol to obtain reference standard solution.

Sample Preparation

ZZHPD samples were prepared according to a previously developed method in our laboratory (Bai et al., 2019). Raw medicinal materials were crushed into pieces and sieved through a 40 mesh sieve before extraction. The ethanol extract of ZZHPD was prepared by reflux extraction method with 75% ethanol two times (1 h each) with the ratio 1:1.2:1 of Zhi-Zi, Hou-Po, and Zhi-

Shi. The two filtrates were mixed and condensed to 1.2 g of raw materials per ml alcohol extract. Then, an accurate amount of 1 ml of the alcohol extract and 79 ml of acetonitrile water (50:50) was mixed and sonicated (250 W, 50 kHz) for 30 min. Afterward, the herbal samples were diluted with acetonitrile water (50:50) to 100 ml volume, aliquoted into 1.5 ml test tubes, and centrifuged twice at high speed of 12,000 rpm for 10 min at 4°C. The supernatant was collected and passed through 0.22 μm filter membrane and injected with 5 μl for UFLC-Q-TOF/MS analysis.

LC-TOF/MS Analysis

LC-MS analysis of ZZHPD was implemented on a Shimadzu UFLC 20ADXR instrument matched with a SIL-20AD-XR automatic sampler, CTO-20AC column oven, and 20AD-XR binary pump, and liquid chromatographic analysis was performed using an Agilent ZORBAX SB-C₁₈ column (5 μm, 250 mm × 4.6 mm i.d.). The mobile phase, consisting of acetonitrile (component A) and 0.1% formic acid water solution (component B), was run at the rate of 1 ml/min. A gradient elution process is as follows: 2–12% A (0–20 min), 12–20% A (20–40 min), 20–28% A (40–50 min), 28–62% A (50–70 min), and 62–64% A (70–80 min). The column temperature was maintained at 40°C throughout the separation process. In addition, an AB SCIEX Triple

TOF™ 5600 equipment (Foster City, CA, United States) coupled with a mass spectrometer with electrospray ion source (ESI) was used for qualitative analysis for ZZHPD. The mass spectrometer was operated in both positive and negative ion modes with dynamic background subtraction, high sensitivity modes, and trigger information-dependent acquisition. The parameters of scan mode were set as follows: auxiliary gas 60 psi, nebulizer gas 60 psi, curtain gas 35 psi, ion source temperature 600°C, and spray voltage 4.5 kV in the positive mode and 4 kV in the negative mode. The ESI mass spectra were acquired in full-scan mode from 50 to 1,500 Da. The Peak View™ Software V.2.0 (Foster City, CA, United States) was used for all the data acquisition and analysis.

Determination of ZZHPD

The quantitative analysis was performed on an Agilent 1100 system equipped with quaternary pump, autosampler injector, and diode array detector. The chemical compositions were separated on a ZORBAX SB-C₁₈ chromatographic column (250 mm × 4.6 mm, 5 μm). The mobile phase was composed of acetonitrile and 0.1% formic acid water as above gradient elution. The flow rate and chromatographic column temperature were set at 1.0 ml/min and 40°C, respectively. The detection wavelength was set at 254 nm and the injection volume was set at 10 μl.

Identification of Chemical Composition

A database containing the information on the chemical composition of raw materials of ZZHPD was established. The database included the compound names, molecular weight, compound formulae, and compound structures retrieving from the databases including TCMSP (<https://tcmsp.com/tcmsp.php>) (Guo et al., 2020), PubMed (<https://www.ncbi.nlm.nih.gov/pubmed>), Web of Science (<http://apps.webofknowledge.com>), and PubChem (<https://www.ncbi.nlm.nih.gov/pccompound>) databases. The reference solutions were used to obtain MS/MS fragment ions and retention time under the above-mentioned mass spectrometry conditions, and the unknown compounds were analyzed and identified using the XIC Manager function build in the PeakView software by referring to the established database and literature retrieval.

Prediction of Potential Targets and Screening of Depression-Related Targets

PubChem database (<https://pubchem.ncbi.nlm.nih.gov/>) was been utilized to collect the canonical SMILES of these components and was used to foreshadow their molecular targets on the Swiss Target Prediction platform (www.swisstargetprediction.ch/) (Gao et al., 2020). Putative targets were further verified by using the UniProt database (<https://www.uniprot.org/>). Depression-related targets were obtained by using the keyword “Depression” in the GeneCards (www.genecards.org/) and OMIM databases (www.omim.org/) (Jiang et al., 2020).

Construction of Component-Target Network and Protein-Protein Interaction (PPI)

Component-target network was established by inputting these potential targets of 31 identified components into the Cytoscape software (version 3.7.1) (Xie et al., 2021). PPIs were discerned utilizing the STRING database (<https://string-db.org/>) (Zhai et al., 2019). Potential target proteins for the antidepressant components of ZZHPD were imported into this STRING database by selecting “Homo sapiens” proteins only. The final result was saved in TSV format and input into the Cytoscape software for the construction of PPI mapping.

Pathway Analysis

The Database for Annotation, Visualization, and Integrated Discovery (DAVID) (Shen et al., 2020) (<https://david.ncifcrf.gov/summary.jsp>) was employed for gene ontology (GO) and Kyoto encyclopedia of genes and genomes (KEGG) pathway enrichment analyses of the corresponding targets of each of the identified ZZHPD components. The threshold of $p < 0.05$ was set, the top 20 of biological processes or pathways were selected and imported into the RStudio software for plotting data, and the top 20 pathways were selected to construct the target-pathway network and associated target proteins to import into the Cytoscape software. The KEGG Mapper software (https://www.kegg.jp/kegg/tool/map_pathway1.html) was used to obtain the antidepressant pathway mapping of the ZZHPD.

Animals and Treatment

Healthy Sprague-Dawley rats (150~200 g, certificate number SCXK-(SU) 2014-000) were provided by the Animal Experimental Center of Nantong University (Nantong University). Experimental rats were fed on a 12 h light/dark cyclic lighting schedule in controllable temperature and humidity conditions, with *ad libitum* access to food and water. After 7 days of acclimatization, the rats were randomly assigned into six groups (8 rats per group), i.e., control group, corticosterone group (CORT group), corticosterone plus 3 g/kg ZZHPD (CZ-3 g/kg), corticosterone plus 6 g/kg ZZHPD (CZ-6 g/kg), corticosterone plus 12 g/kg ZZHPD (CZ-12 g/kg), and corticosterone plus 20 mg/kg fluoxetine group (CF-20 mg/kg). As previously described, CORT was administered subcutaneously to induce depression at 20 mg/kg once daily for 21 days (Bai et al., 2018). ZZHPD and fluoxetine were orally administrated each day 30 min prior to the corticosterone injection.

Body Weight Test

Rat body weight was recorded on days 7, 14, and 21 after the initiation of ZZHPD treatment. The rats were weighed by an electronic scale and the average values of the two measurements were recorded.

Sucrose Preference Test

An SPT was performed to evaluate anhedonia based on the animal's natural preference for sweets (Liu et al., 2018). All rats in each group were trained to adapt to 1% sucrose

TABLE 1 | MRM parameters of 5-HT, DA and internal standards (IS).

Analyte	Precursor ion (m/z)	Product ion (m/z)	Dwell time (ms)	DP (V)	CE (ev)	CXP (V)
5-HT	177.1	160.1	50	130	17	16
DA	154.1	137.1	50	52	17	14
IS	212.2	194.1	50	130	14	14

solution in two bottles on the 18th day of the experiment and replace a bottle of sucrose solution with fresh water on the 19th day. After the adaptability, water and food were deprived for 12 h, the SPT lasted 4 h (14:00–18:00), and the positions of two bottles were exchanged at 16:00. Sucrose preference was calculated using the formula as follows:

Sucrose preference (%) = Sucrose consumption (ml)/[Water (ml) and Sucrose consumption (ml)] × 100% (Ali et al., 2015).

Forced Swim Test

An FST was done as the previous description but with slight modification (Bahi et al., 2014). In brief, on day 21 of the experiment, rats were put into a cylindrical red plastic bucket filled with 30 cm high room temperature water. The test lasted 6 min and during the last 4 min, and each rat was forced to swim without touching the bottom of the bucket. The water was changed with fresh water after every test to reduce the interference from previous tests.

Hippocampal Samples Collection and cAMP Level

After forced swim test, the rats were euthanized under anesthesia with chloral hydrate. After draining the blood from the abdominal aorta, the whole brain tissue was removed, and the blood on the brain surface was washed with a precooled phosphate-buffered saline solution. Then, these bilateral hippocampi were isolated on an ice bag and stored at -80°C . The concentrations of cAMP in the hippocampal samples were detected using a commercial ELISA kit according to the manufacturer's instructions (Nanjing Jiancheng Bioengineering Institute, Nanjing, Jiangsu, China).

LC-MS/MS for 5-HT and Dopamine Levels

The levels of 5-HT and DA in the hippocampal samples were analyzed using an AB Sciex QTRAP 5500 coupled to a Prominence™ UFLC system under a multiple reaction monitoring (MRM) mode. Chromatography was selected on a Waters XBridge BEH amide column (3.5 μm , 2.1 mm × 100 mm i.d.) according to the preexperiment results. The mobile phase consisted of pump A (0.2% formic acid acetonitrile) and pump B (0.2% formic acid solution) with a flow rate of 0.8 ml/min. The gradient elution program was as follows: 0–4 min, 95–50% A; 4–8 min, 50–95% A; 8–9 min, 95–95% A. The injection volumes were 1 μl for 5-HT and DA. The optimal operation conditions were as follows: source temperature (TEM), 550°C ; spray voltage, 5,000 V; curtain gas (CUR), 35 psi; ion source gas 1 (GS 1), 55 psi; heater gas (GS 2), 55 psi. The Q1, Q3, declustering potential (DP),

TABLE 2 | The primers for RT-PCR.

Genes	Forward primer (5-3')	Reverse primer (5-3')
MAOA	ACTGCTCGGGAATTTGCGTA	CAAAATTCGTTCTCTGGCCG
MAOB	GGGACAGAGTGAAGCTGGAG	CCCAAGGCACACGAGTAAT
DRD2	CATTGTCTGGGTCCTGTCTCT	GACCAGCAGAGTGACGATGA
CREBBP	ATCCCATAGACCCAGTTCC	CGGCTGCTGATCTGTTGTTA
AKT1	ACTCATTCCAGACCCACGAC	CCGGTACACCACGTTCTTCT
MAPK1	TCTCCCGCACAAAATAAGG	GCCAGAGCCTGTTCAACTTC
HTR1A	TGTTGCTCATGCTGGTTCTC	CCGACGAAGTTCCTAAGCTG
GRIN2B	GTGAGAGCTCCTTTGCCAAC	TGAAGCAAGCACTGGTCATC
β -Actin	AGCCATGTACGTAGCCATCC	CTCTCAGCTGTGGTGGTAA

dwell time (DT), collision cell exit potential (CXP), and collision energy (CE) values of 5-HT, DA, and isoproterenol (internal standard, IS) were optimally selected by Applied Biosystems/MDS Sciex Analyst software (version 1.5.2). The MRM transitions at 177.1 → 160.1, 154.1 → 137.1, and 212.2 → 194.1 were selected to analyze 5-HT, DA, and IS, and the suitable multiple reaction monitoring values are listed in **Table 1**.

Hippocampal tissues were accurately weighed and homogenized in PBS solution. These samples were centrifuged at high speed of 12,000 rpm after vortexing for 3 min. 50 μl supernatant was placed in an EP tube, and then 150 μl of 1% formic acid in acetonitrile containing 800 ng/ml isoproterenol was also added and vortex-mixed thoroughly for 3 min. After another high-speed centrifugation, 100 μl aliquot of the solution was transferred to an autosampler vial and analyzed using LC-MS/MS system.

Quantitative RT-qPCR Analysis

The total mRNA was extracted from the hippocampal tissues using TRIzol following the instructions provided by the manufacturer. RNA purity between 1.8 and 2.1 was considered acceptable as indicated by the ratio of absorbance at 260 and 280 nm using a UV spectrophotometer. RNA was reverse-transcribed to cDNA carried out using the PrimeScript RT reagent kit (TaKaRa) with gDNA Eraser. The reaction was performed on an ABI StepOnePlus Real-Time PCR System. The PCR programs are as follows 95°C for the 30 s, 95°C for 5 s, and 60°C for 60 s. Forty cycles of PCR were performed, and relative gene expression levels were calculated using the $2^{-\Delta\Delta\text{Ct}}$ method after normalization to β -actin. The primer sequences are shown in **Table 2**.

Western Blot Analysis

Total proteins were extracted from the hippocampal tissue using RIPA lysis buffer containing 1× protease and phosphatase

TABLE 3 | Compounds identified in the alcohol extracts of ZZHPD by UFLC-TOF/MS.

Peak no.	RT (min)	Adduct	Extraction mass (Da)	Found mass (Da)	Error (ppm)	MS/MS	Formula	Identification	Origin
1	2.68	+H	168.10191	168.1018	-0.9	150, 135, 107, 91	C ₉ H ₁₃ NO ₂	Synephrine*	ZS
2	11.41	-H	391.12459	391.12322	-3.5	229, 211, 193, 167, 149	C ₁₆ H ₂₄ O ₁₁	Shanzhiside (Wu H. et al., 2015)	ZZ
3	11.94	-H	373.11402	373.11209	-5.2	211, 193, 167, 149, 123	C ₁₆ H ₂₂ O ₁₀	Geniposidic acid*	ZZ
4	13.16	-H	403.12459	403.12221	-5.9	241, 223, 191, 139	C ₁₇ H ₂₄ O ₁₁	Deacetyl asperulosidic acid methyl ester (Wang et al., 2015)	ZZ
5	14.2	-H	389.10894	389.10669	-5.8	345, 183, 139	C ₁₆ H ₂₂ O ₁₁	Deacetylasperulosidic acid*	ZZ
6	14.35	-H	403.12459	403.12209	-6.2	371, 241, 223, 127	C ₁₇ H ₂₄ O ₁₁	Gardenoside (Wu H. et al., 2015)	ZZ
7	15.41	-H	405.14024	405.13759	-6.5	359, 197, 153	C ₁₇ H ₂₆ O ₁₁	Shanzhiside methylester (Yue et al., 2013)	ZZ
8	15.73	-H	403.12459	403.12328	-3.2	241, 223, 139	C ₁₇ H ₂₄ O ₁₁	Feretoside (Wang et al., 2015)	ZZ
9	19.17	-H	353.08781	353.08624	-4.4	191	C ₁₆ H ₁₈ O ₉	Chlorogenic acid*	ZZ
10	20.9	-H	549.18249	549.17963	-5.2	225, 207, 123	C ₂₃ H ₃₄ O ₁₅	Genipin 1-gentiobioside*	ZZ
11	21.04	-H	179.03498	179.03486	-0.7	135	C ₉ H ₈ O ₄	Caffeic acid*	ZZ
12	24.18	-H	387.12967	387.12733	-6.1	225, 207, 147	C ₁₇ H ₂₄ O ₁₀	Geniposide*	ZZ
13	24.19	-H	225.07685	225.07675	-0.4	207, 147, 101	C ₁₁ H ₁₄ O ₅	Genipin (Jia et al., 2019)	ZZ
14	34.88	+H	611.16066	611.1601	-1	303	C ₂₇ H ₃₀ O ₁₆	Rutin*	ZZ
15	40.02	+H	581.18648	581.1853	-2	419, 273, 435	C ₂₇ H ₃₂ O ₁₄	Narirutin (Ma et al., 2011)	ZS
16	42.16	+H	581.18648	581.1855	-1.6	273, 153	C ₂₇ H ₃₂ O ₁₄	Naringin*	ZS
17	42.99	-H	577.15628	577.14988	-1.1	269, 577	C ₂₇ H ₃₀ O ₁₄	Rhoifolin (Li et al., 2013)	ZS
18	44.07	+H	611.19705	611.1954	-2.7	465, 449, 303, 413	C ₂₈ H ₃₄ O ₁₅	Hesperidin*	ZS
19	45.79	+H	611.19705	611.1954	-2.8	465, 449, 303	C ₂₈ H ₃₄ O ₁₅	Neohesperidin*	ZS
20	54.04	+H	595.20213	595.2004	-2.9	287, 153	C ₂₈ H ₃₄ O ₁₄	Poncirin (Ma et al., 2011)	ZS
21	56.84	-H	271.0612	271.05906	-7.9	177, 151, 119	C ₁₅ H ₁₂ O ₅	Naringenin (Li et al., 2013)	ZS
22	60.91	+H	373.12818	373.1274	-2.1	358, 343, 315, 181	C ₂₀ H ₂₀ O ₇	Isosinensetin (Wang et al., 2007)	ZS
23	61.68	+H	217.04954	217.0492	-1.5	202, 174, 146	C ₁₂ H ₈ O ₄	Bergapten (Liao et al., 2018)	ZS
24	62.43	+H	473.21699	473.2156	-3.1	369, 187, 161	C ₂₆ H ₃₂ O ₈	Deacetylnomilin (Tian and Schwartz, 2003)	ZS
25	63.2	+H	373.12818	373.1273	-2.3	357, 343, 315	C ₂₀ H ₂₀ O ₇	Sinensetin (Wang et al., 2007)	ZS
26	63.73	+H	471.20134	471.2001	-2.6	425, 161	C ₂₆ H ₃₀ O ₈	Limonin (Tian and Schwartz, 2003)	ZS
27	65.61	+H	403.13874	403.1376	-2.7	388, 373, 358, 330	C ₂₁ H ₂₂ O ₈	Nobiletin (Wang et al., 2007)	ZS
28	66.05	+H	515.22756	515.2255	-4.1	469, 161	C ₂₈ H ₃₄ O ₉	Nomilin (Cai et al., 2016)	ZS
29	68.32	+H	373.12818	373.1271	-2.8	358, 343, 328, 300	C ₂₀ H ₂₀ O ₇	Tangeretin (Wang et al., 2007)	ZS
30	71.07	+H	267.13796	267.137	-3.5	239, 226, 197, 165	C ₁₈ H ₁₈ O ₂	Honokiol*	HP
31	74.03	+H	267.13796	267.1372	-2.7	239, 226, 197, 165	C ₁₈ H ₁₈ O ₂	Magnolol*	HP

* Identifications confirmed with standard compound. Notes: HP, Magnolia officinalis; ZZ, Gardenia jasminoides; ZS, Citrus × aurantium.

inhibitor cocktail. The proteins were loaded on a 12% SDS-PAGE gel and transferred onto 0.45 μm PVDF membrane (Millipore, Billerica, MA, United States). After blocking with 5% nonfat dried milk for 1 h at room temperature, the membranes were incubated with BDNF (1:1,000; Abcam, Cambridge, MA, United States), PKA (1:2,000; CST, Danvers, MA, United States), CREB (1:2,000; CST, Danvers, MA, United States), and p-CREB (1:2,000; CST, Danvers, MA, United States) approximately 12 h at 4°C. Subsequently, the membranes were rinsed thrice with PBS/0.1% Tween-20 (PBST) and then exposed to secondary antibodies 1 h at room temperature. The protein blots were washed with PBST, and immunoreactive signals were visualized by enhanced chemiluminescence equipment. The band densities of the proteins were measured by Image Lab software (Bio-Rad Laboratories, Hercules, CA, United States).

Statistical Analyses

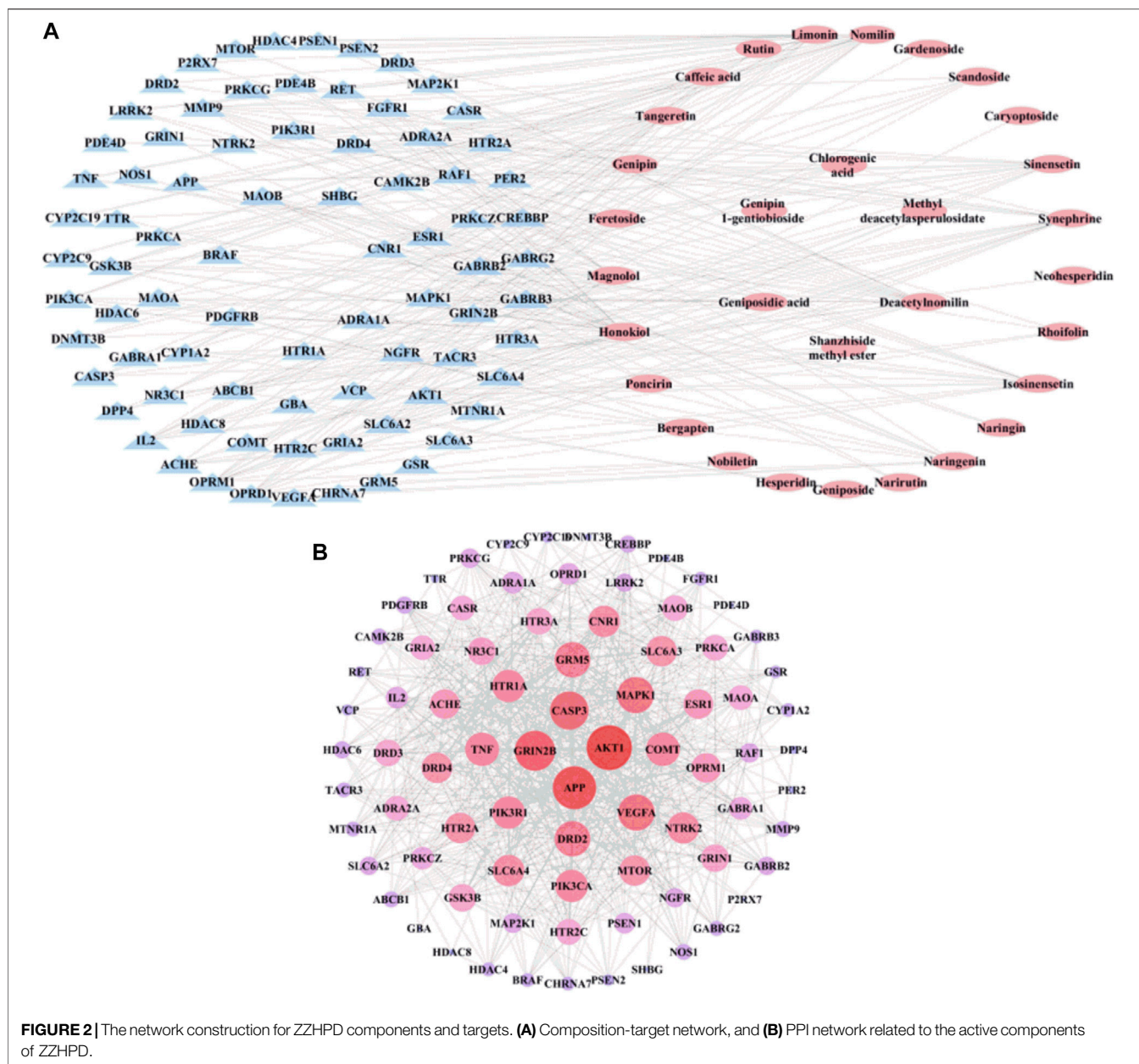
SPSS 18.0 (IBM, Chicago, IL, United States) was used for testing the differences between multiple groups by ANOVA. A value of $p < 0.05$ was considered statistically significant. Figures were

prepared using GraphPad Prism 6.0 software (San Diego, CA, United States).

RESULTS

Ingredient Identification of ZZHPD Based on LC-TOF/MS

In order to obtain the high sensitivity and optimized chromatographic conditions of alcohol extracts of ZZHPD, several mobile phase systems including methanol-0.1% formic acid water, acetonitrile-0.1% formic acid water, methanol-water, and acetonitrile water were selected. The results showed that acetonitrile water with 0.1% formic acid had the best separation and abundant signal response regardless of positive and negative ion scanning modes in the optimized gradient mode. Total ion chromatograms of alcohol extracts of ZZHPD in the positive and negative ion modes are represented in **Supplementary Figure S1**, and the extracted ion chromatographs (EIC) of the qualitative samples of ZZHPD are presented in **Supplementary Figures S2–S32**. In light of the chromatographic peak retention time,



relative molecular mass, typical fragment ions, and structural characteristics, as well as comparison to the reference standards and literature searching, a total of 31 compounds were identified in ZZHPD samples. Of them, 13 compounds were unambiguously confirmed by matching the retention time and fragment ions between the samples and reference chemicals. In addition, the data of ZZHPD compounds including retention time, extraction mass, error values, and MS/MS fragment ion were used to analyze the structure of unknown chemical composition, as shown in **Table 3**.

Quantitative Analysis of Seven Compounds

As shown in **Supplementary Figure S33**, seven compounds in ZZHPD showed a peak shape and reached better baseline

separation in 80 min under optimum conditions. They were genipin 1-gentiobioside 2.45 mg/g, geniposide 12.32 mg/g, naringin 21.90 mg/g, hesperidin 1.77 mg/g, neohesperidin 22.17 mg/g, honokiol 1.49 mg/g, and magnolol 4.44 mg/g in ZZHPD.

Predicted Targets and Component-Target Network

To understand the pharmacological activities of the identified components in the alcohol extracts, potential molecule targets of these components were predicted using the Swiss Target Prediction platform (Gu et al., 2020; Zhang et al., 2020). A total of 1,484 putative targets closely related to 31 identified

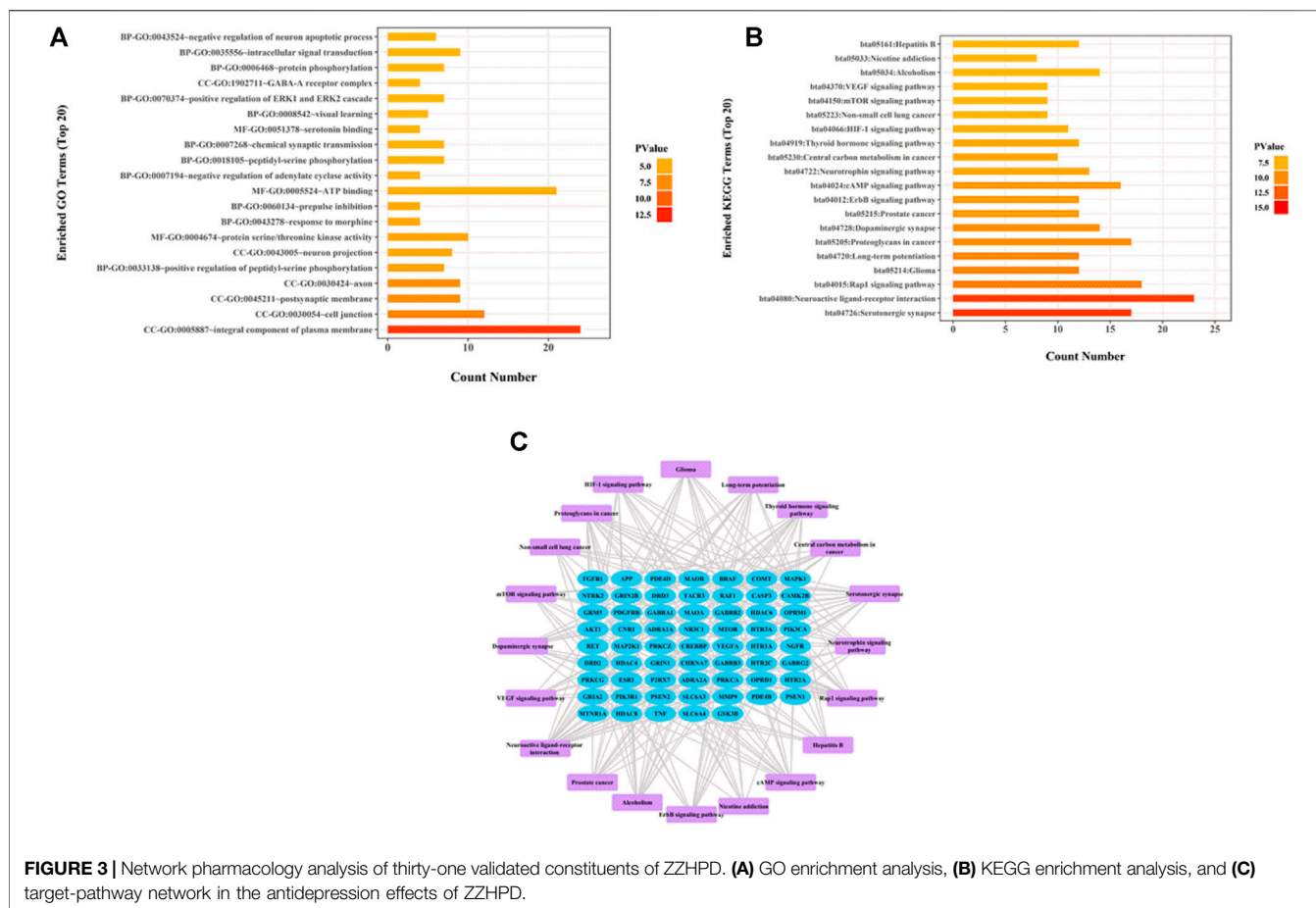


FIGURE 3 | Network pharmacology analysis of thirty-one validated constituents of ZZHPD. **(A)** GO enrichment analysis, **(B)** KEGG enrichment analysis, and **(C)** target-pathway network in the antidepressant effects of ZZHPD.

components were retrieved, and 514 targets were finally obtained after removing duplicates (**Supplementary Table S1**). Furthermore, 527 depression-related target genes were pinpointed by the GeneCards and OMIM databases after deleting duplicates. By comparing these depression-related target genes, 80 genes that may be involved in the antidepressant activity of ZZHPD were recorded. **Figure 2A** shows the component-target network diagram generated by the Cytoscape software. The network involved 31 chemical components, 80 targets, 111 nodes, and 242 edges. The network characteristics included the network density of 0.040, the characteristic path length of 3.295, an average number of adjacent nodes of 4.360, the network heterogeneity of 1.114, and the network centrality of 0.210. The chemical components with a higher degree value were honokiol (degree = 27), deacetylnomilin (degree = 21), nomilin (degree = 21), magnolol (degree = 18), synephrine (degree = 17), and limonin (degree = 17), indicating that these components are important for the therapeutic effect of ZZHPD on depression.

PPI Network

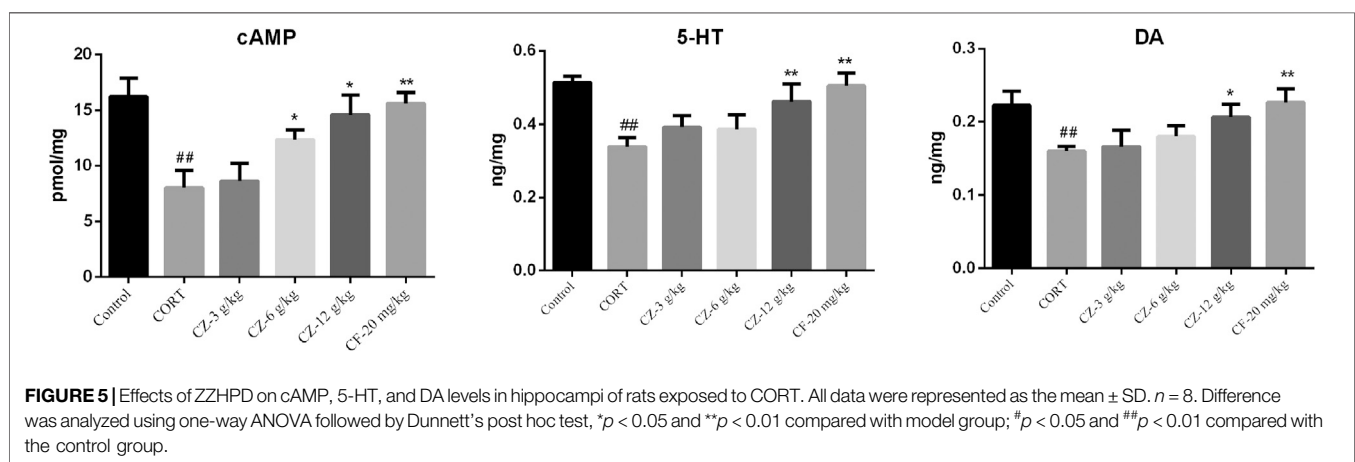
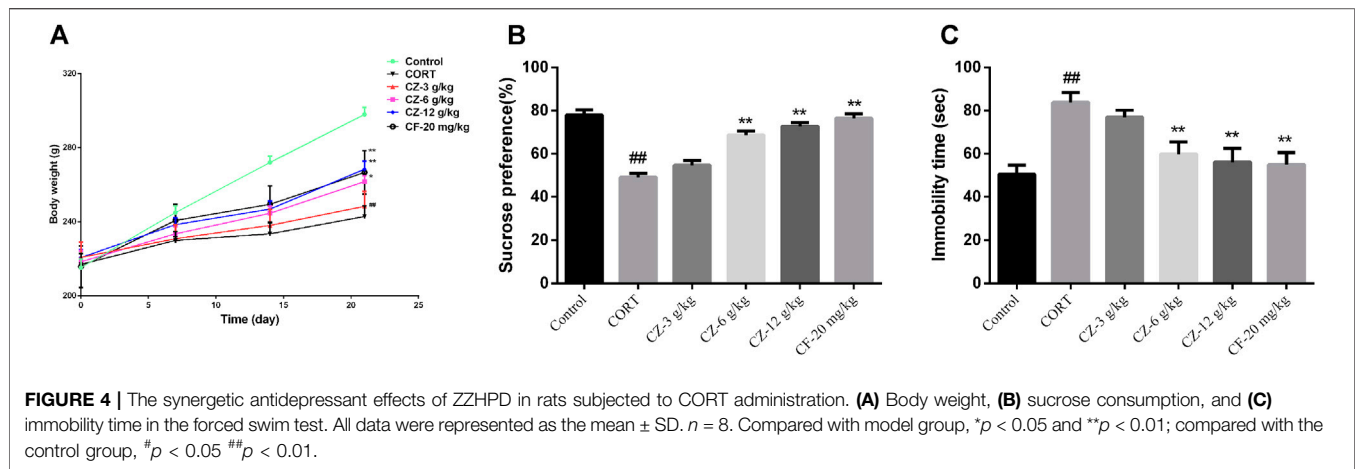
To further explore the complex mechanism of action of ZZHPD, the PPI relationship was further evaluated by using the Cytoscape software and STRING database to create a PPI network. As shown in **Figure 2B**, the constructed PPI network had 80 targets, 80 nodes, and 700 edges. The size of the node degree value is indicated by the size and color of the nodes; that is, the bigger the node and

the closer the color to red, the higher the node degree value. The results showed the network density of 0.222, the characteristic path length of 1.95, an average number of adjacent nodes of 17.5, the network heterogeneity of 0.542, and the network centrality of 0.305. The node degrees of the genes, AKT1, APP, GRIN2B, CASP3, VEGFA, MAPK1, GRM5, and DRD2, were greater than 30, suggesting that these genes as potential targets are involved in the treatment of depression with ZZHPD.

Gene Function and Pathway Analysis

To test whether active components in the alcohol extracts of ZZHPD can modulate target gene-related signaling pathways, DAVID online database was utilized to analyze GO and KEGG pathway enrichment in the biological system networks (Ou et al., 2020). **Figures 3A,B** showed the enriched GO and KEGG analyses of 80 target genes of 31 active components, respectively (**Supplementary Tables S2, S3**). The top 20 biological processes or pathways were analyzed and shown. By importing the first 20 KEGG pathways and associated target proteins into the Cytoscape software, the target-pathway network was generated (**Figure 3C**).

GO enrichment analysis revealed three aspects: cellular components, molecular functions, and biological processes. Cellular components were mostly related to the integral component of plasma membrane, postsynaptic membrane,



axon, neuron projection, and GABA-A receptor complex. The biological processes mainly included the positive regulation of peptidyl-serine phosphorylation, prepulse inhibition, negative regulation of adenylate cyclase activity, chemical synaptic transmission, protein phosphorylation, and intracellular signal transduction. Molecular functions were chiefly associated with serine/threonine kinase activity, ATP binding, and serotonin binding protein. KEGG analysis indicated the pathways predominantly involved in the antidepressant effects of ZZHPD, including serotonergic synapse, neuroactive ligand-receptor interaction, dopaminergic synapse, cAMP signaling pathway, and mTOR signaling pathway.

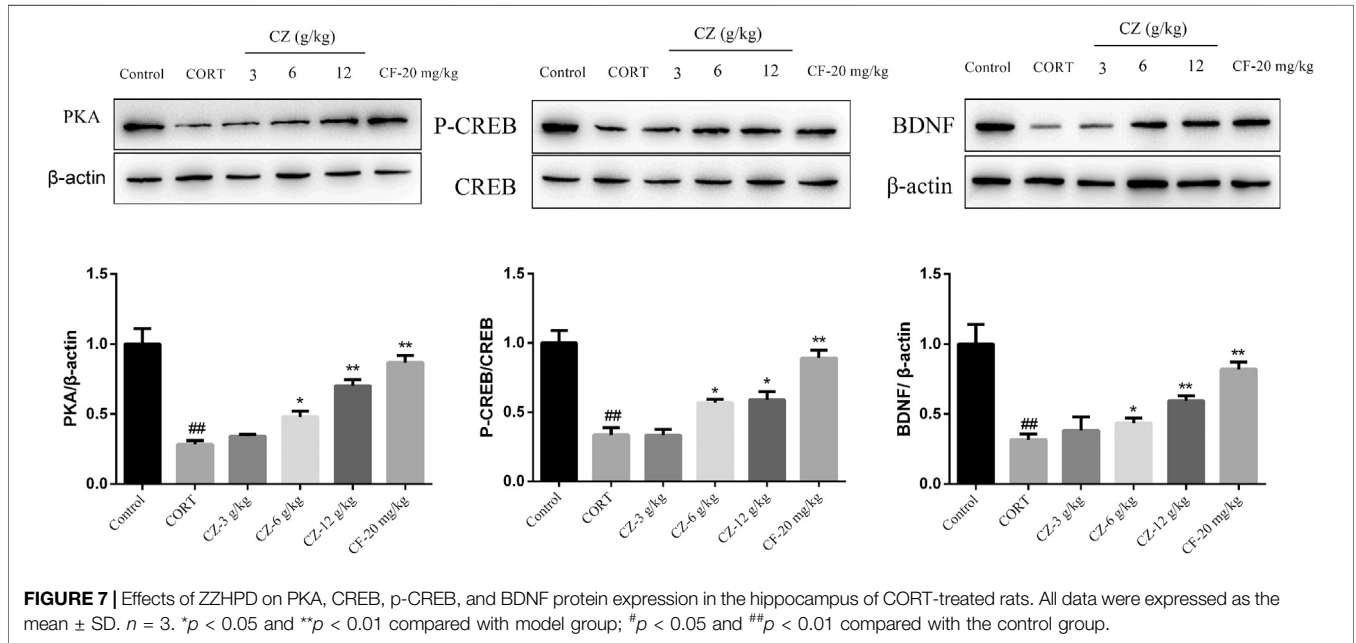
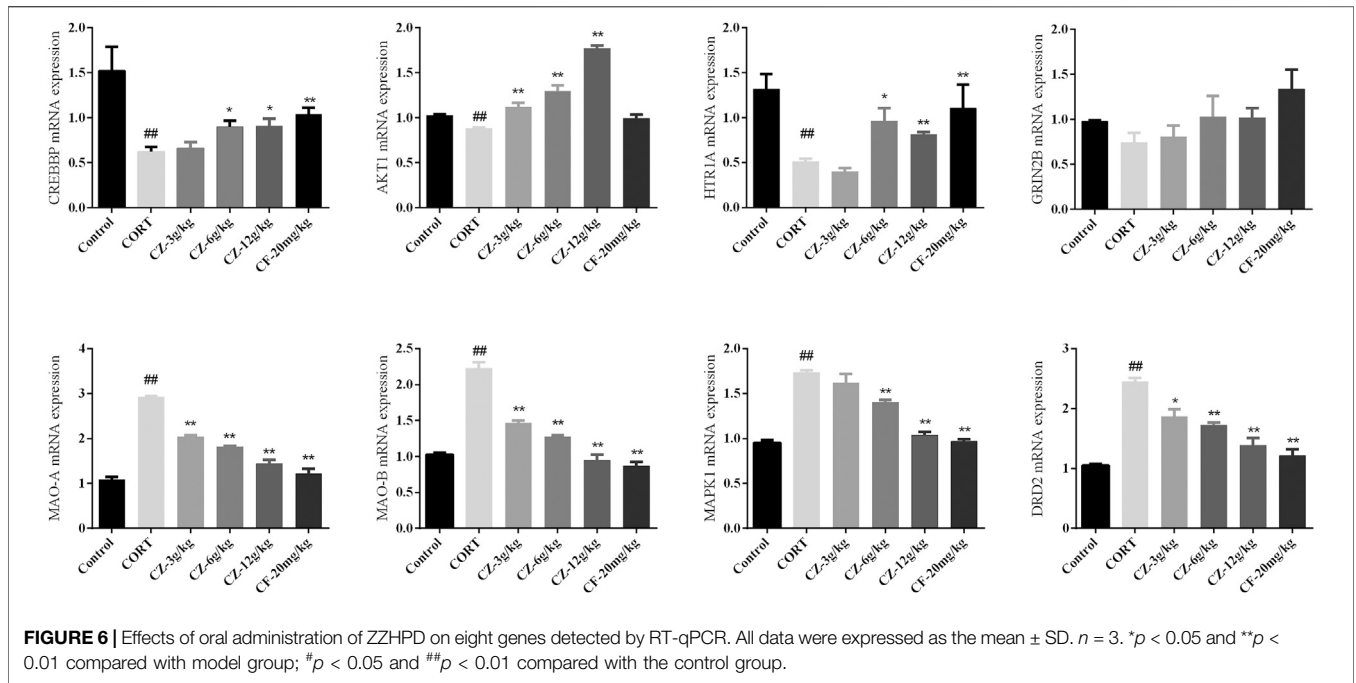
Effects of ZZHPD on Body Weight, Sucrose Preference Test, and Forced Swim Test

After subcutaneous injection of CORT for 21 consecutive days, the model group showed obvious depressive behavior. Compared with the control group, the CORT group had a marked reduction in body weight and sucrose intake rate ($P_s < 0.01$) and a significantly longer immobility time during the FST experiment ($p < 0.01$), indicating that the CORT-induced

depression model was successfully constructed. The ANOVA test showed that ZZHPD produced significant effects on SPT and FST in rats. As shown in **Figure 4**, ZZHPD treatment at the doses of 6 and 12 g/kg/d ($P_s < 0.01$) significantly increased body weight and sucrose uptake rate ($P_s < 0.01$). In addition, ZZHPD decreased the immobility time of FST versus the CORT group.

Effects of ZZHPD on cAMP, 5-HT, and Dopamine Levels of Hippocampus

Varying cAMP levels in hippocampal tissue were shown in **Figure 5**. ZZHPD at a low dose (3 g/kg) had no effect on cAMP levels, while medium and high doses of ZZHPD (6 and 12 g/kg; $P_s < 0.05$) significantly increased the cAMP levels in the hippocampus compared with the model group. As expected, the positive control (fluoxetine) significantly increased the cAMP levels ($p < 0.01$). Hippocampal 5-HT and DA levels in the model group were significantly lower than those in the control group, but they were significantly increased following ZZHPD treatment at a high dose of ZZHPD ($p < 0.05$). In addition, elevated levels of 5-HT and DA were observed with fluoxetine treatment ($P_s < 0.01$).



RT-qPCR Detection of Related Gene Expression

The results of RT-qPCR indicated that the expression levels of CREBBP, AKT1, and HTR1A were significantly lower, while those of MAOA, MAOB, DRD2, and MAPK1 were higher in the model group than in the control group. As shown in Figure 6, the group undergoing ZZHPD treatment showed a marked increase in CREBBP, AKT1, and HTR1A mRNA levels. Meanwhile, the mRNA levels expression of MAOA, MAOB,

DRD2, and MAPK1 in the ZZHPD-treated group were significantly attenuated compared with those in the CORT group.

Effects of ZZHPD on Protein Expression of PKA, BDNF, and p-CREB

In order to further explore the antidepressant mechanism of ZZHPD, cAMP signaling pathway was studied by detecting the protein expression levels of PKA and BDNF and the

phosphorylation status of CREB by WB. As shown in **Figure 7**, the model group rats showed marked downregulation of the expression levels of PKA, BDNF, and phosphorylated CREB compared with the control group. Meanwhile, the protein expression levels of PKA, p-CREB, and BDNF increased significantly following treatment with medium and high doses of ZZHPD.

DISCUSSION

MDD has complex and multifactorial etiology related to psychological, physical, emotional, and social impairment (Leubner and Hinterberger, 2017; Li et al., 2021). At present, effective treatments for depression are very limited, and TCM is gaining more attention for the clinical therapy of depression (Wang et al., 2019). However, the clinical effects of TCM are inconsistent and difficult to evaluate due to variable composition resulting from a nonstandard preparation process in certain settings. Moreover, the efficacy of TCM depends largely on the combination of multiple active compounds, rather than on any single individual ingredient. These issues pose a big challenge for the evaluation of the clinical efficacy of TCM and for understanding of the material basis and molecular mechanisms responsible for its therapeutic efficacy. Fortunately, network pharmacology has evolved from systems biology and multidirectional pharmacology, thus revolutionizing the practice of TCM by shifting the paradigm of “one drug, one target, one disease” towards the model of “multicomponent, multitarget, multidisease,” therefore making it possible to uncover the complex relationship between active components and their targets (Wang J. et al., 2018; Yu et al., 2018; Sun et al., 2021).

ZZHPD is an effective TCM formula used for the treatment of depression. Yao et al. utilized FST and TST to assess the antidepressant effect of ZZHPD after the last administration. The results demonstrated that the antidepressant-like mechanism of ZZHPD was related to the monoaminergic system (Yao et al., 2013). However, the chemical composition and the interactions of herbs in ZZHPD during decoction are unclear. Liu et al. developed an effectively integrated method based on HPLC-MS coupled with chemometrics to identify the compounds in ZZHPD and to reveal the potential physicochemical changes during decoction (Liu et al., 2016). Our study used the UFLC-Q-TOF/MS to identify the chemical composition of alcohol extracts of ZZHPD and mined the potential mechanism in the treatment of depression using network pharmacology. By network analysis, our study obtained an initial understanding of potential molecular targets, major signaling pathways, important regulatory processes, and associated cellular components in the treatment of depression with ZZHPD by network analysis. More specifically, the analysis of network pharmacology data suggested that the antidepressant effects of ZZHPD were largely mediated by the regulation of the cAMP signaling pathway and 5-HT/DA synaptic transmission. Indeed, the cAMP/PKA/BDNF signaling pathway is one of the most important signaling pathways involved in antidepressant therapy. cAMP could mediate the

protein kinase A-cAMP response element-binding (CREB) signaling pathway as an important second messenger (Wang X. L. et al., 2018). CREB, an important transcriptional element necessary for the survival of neurons, is mainly activated at a particular residue, serine 133 (Ser133). And BDNF is the major transcriptional product of CREB phosphorylation (Chen et al., 2019; Yu et al., 2021), which acts on certain neurons of the central nervous system to support the survival of existing neurons and encourage the growth and differentiation of new neurons and synapses (Kim et al., 2017; Bai et al., 2018). Meanwhile, preclinical and clinical trials have indicated that the related proteins of cAMP/PKA/CREB are downregulated in depression and upregulated by antidepressant therapy (Li et al., 2009; Fujita et al., 2017; Lian et al., 2018).

In addition, several key components including magnolol, synephrine, honokiol, and limonin, may largely contribute to the antidepressant efficacy of ZZHPD by network pharmacology analysis. These active compounds share similar pharmacological effects, although each has unique biological activities. For example, magnolol—the main component of *Magnolia officinalis*—has antioxidative, antitumor, and antidepressant effects *via* suppressing neuroinflammation and decreasing the levels of p-ERK, GSK3 β , and Smad (Cheng et al., 2018; Chei et al., 2019), synephrine has antitumor and antidepressant properties through inhibition of Galectin-3-AKT/ERK signaling and the stimulation of α 1 adrenoceptors (Song et al., 1996; Xu et al., 2018), and honokiol has been proven to protect against inflammation and depression *via* suppressing the activation of TXNIP-NLRP3 inflammasome and NF- κ B signaling pathway, reducing the levels of related proinflammatory cytokines (Tang et al., 2018; Xia et al., 2019; Zhang B. et al., 2019), while limonin has been recognized to have a medicinal value with antioxidant and tumor-inhibiting capacities (Brekša and Manners, 2006; Su et al., 2019). Therefore, the above-mentioned literature supports the idea that these natural products are thought to work synergistically to endow ZZHPD with effective antidepressant effects.

In animal behavior experiments, including body weight test, SPT, and FST, ZZHPD showed antidepressant effects after 3 weeks of treatment. Notably, ZZHPD effectively regulated MAOA, MAOB, DRD2, CREBBP, AKT1, MAPK1, and HTR1A mRNA levels and upregulated BDNF expression by the cAMP signal pathway, involving the phosphorylation of transcription factor CREB. Meanwhile, hippocampal 5-HT and DA contents were obviously improved with ZZHPD treatment. These findings were in accordance with the predictive results derived from the network analysis.

CONCLUSION

This study systematically evaluated the antidepressant mechanism of ZZHPD by network pharmacology analysis and experimental verification. UFLC-Q-TOF/MS-based analytical tool was used to profile the phytochemicals of ZZHPD, resulting in the identification of a total of 31 active compounds in the alcohol extracts of ZZHPD. The KEGG pathway enrichment indicated that the antidepressant

mechanism of ZZHPD was mainly involved in the dopaminergic synapse, serotonin synapse, and cAMP signaling pathway. The subsequent *in vivo* experiments verified that the antidepressant mechanism of ZZHPD was consistent with the predictions of network pharmacology. In conclusion, we demonstrated that the antidepressant mechanism of ZZHPD is based on multicomponent, multitarget, and system regulation.

DATA AVAILABILITY STATEMENT

The raw data supporting the conclusion of this article will be made available by the authors, without undue reservation, to any qualified researcher.

ETHICS STATEMENT

The animal study was reviewed and approved by the Committee of the Nanjing University of Chinese Medicine. Written informed consent was obtained from the owners for the participation of their animals in this study.

REFERENCES

- Ali, S. H., Madhana, R. M., K V, A., Kasala, E. R., Bodduluru, L. N., Pitta, S., et al. (2015). Resveratrol Ameliorates Depressive-like Behavior in Repeated Corticosterone-Induced Depression in Mice. *Steroids* 101, 37–42. doi:10.1016/j.steroids.2015.05.010
- Bahi, A., Schwed, J. S., Walter, M., Stark, H., and Sadek, B. (2014). Anxiolytic and Antidepressant-like Activities of the Novel and Potent Non-imidazole Histamine H₃ Receptor Antagonist ST-1283. *Drug Des. Devel Ther.* 8, 627–637. doi:10.2147/DDDT.S63088
- Bai, Y., Song, L., Dai, G., Xu, M., Zhu, L., Zhang, W., et al. (2018). Antidepressant Effects of Magnolol in a Mouse Model of Depression Induced by Chronic Corticosterone Injection. *Steroids* 135, 73–78. doi:10.1016/j.steroids.2018.03.005
- Bai, Y., Song, L., Zhang, Y., Dai, G., Zhang, W., Song, S., et al. (2019). Comparative Pharmacokinetic Study of Four Major Bioactive Components after Oral Administration of Zhi-Zi-Hou-Po Decoction in normal and Corticosterone-Induced Depressive Rats. *Biomed. Chromatogr.* 33, e4542. doi:10.1002/bmc.4542
- Banerjee, S., Bhattacharjee, P., Kar, A., and Mukherjee, P. K. (2019). LC-MS/MS Analysis and Network Pharmacology of Trigonella Foenum-Graecum - A Plant from Ayurveda against Hyperlipidemia and Hyperglycemia with Combination Synergy. *Phytomedicine* 60, 152944. doi:10.1016/j.phymed.2019.152944
- Breksa, A. P., 3rd, and Manners, G. D. (2006). Evaluation of the Antioxidant Capacity of Limonin, Nomilin, and Limonin Glucoside. *J. Agric. Food Chem.* 54, 3827–3831. doi:10.1021/jf060901c
- Cai, Y., Zhang, S., Wang, Q., Sun, H., Zhou, M., Hu, S., et al. (2016). A Rapid, Selective and Sensitive UPLC-MS/MS Method for Quantification of Nomilin in Rat Plasma and its Application in a Pharmacokinetic Study. *Planta Med.* 82, 224–229. doi:10.1055/s-0035-1558157
- Chei, S., Oh, H. J., Song, J. H., Seo, Y. J., Lee, K., and Lee, B. Y. (2019). Magnolol Suppresses TGF- β -Induced Epithelial-To-Mesenchymal Transition in Human Colorectal Cancer Cells. *Front. Oncol.* 9, 752. doi:10.3389/fonc.2019.00752
- Chen, Q., Ma, H., Guo, X., Liu, J., Gui, T., and Gai, Z. (2019). Farnesoid X Receptor (FXR) Aggravates Amyloid- β -Triggered Apoptosis by Modulating the cAMP-Response Element-Binding Protein (CREB)/Brain-Derived Neurotrophic Factor (BDNF) Pathway *In Vitro. Med. Sci. Monit.* 25, 9335–9345. doi:10.12659/MSM.920065

AUTHOR CONTRIBUTIONS

YB and WJ contributed to conception and design; YZ and XW performed the network pharmacology analysis; YB, BH, and WZ supervised and wrote the article. SL analyzed the data. All authors reviewed the manuscript and approved the final manuscript.

FUNDING

This study work was financially supported by a grant from the National Natural Science Foundation of China (grant number 81573685), the Special Subject of Chinese Medicine Research in Henan Province (20-21ZY2307), and the Science and Technology Research Project of Henan Province (no. 212102311096).

SUPPLEMENTARY MATERIAL

The Supplementary Material for this article can be found online at: <https://www.frontiersin.org/articles/10.3389/fphar.2021.711303/full#supplementary-material>

- Cheng, J., Dong, S., Yi, L., Geng, D., and Liu, Q. (2018). Magnolol Abrogates Chronic Mild Stress-Induced Depressive-like Behaviors by Inhibiting Neuroinflammation and Oxidative Stress in the Prefrontal Cortex of Mice. *Int. Immunopharmacol* 59, 61–67. doi:10.1016/j.intimp.2018.03.031
- Cheung, F. (2011). TCM: Made in China. *Nature* 480, S82–S83. doi:10.1038/480S82a
- Coupland, C., Hill, T., Morriss, R., Moore, M., Arthur, A., and Hippisley-Cox, J. (2018). Antidepressant Use and Risk of Adverse Outcomes in People Aged 20–64 Years: Cohort Study Using a Primary Care Database. *BMC Med.* 16, 36. doi:10.1186/s12916-018-1022-x
- Dean, J., and Keshavan, M. (2017). The Neurobiology of Depression: An Integrated View. *Asian J. Psychiatr.* 27, 101–111. doi:10.1016/j.ajp.2017.01.025
- Fujita, M., Richards, E. M., Niciu, M. J., Ionescu, D. F., Zoghbi, S. S., Hong, J., et al. (2017). cAMP Signaling in Brain Is Decreased in Unmedicated Depressed Patients and Increased by Treatment with a Selective Serotonin Reuptake Inhibitor. *Mol. Psychiatry* 22, 754–759. doi:10.1038/mp.2016.171
- Gao, Y., Wang, K. X., Wang, P., Li, X., Chen, J. J., Zhou, B. Y., et al. (2020). A Novel Network Pharmacology Strategy to Decode Mechanism of Lang Chuang Wan in Treating Systemic Lupus Erythematosus. *Front. Pharmacol.* 11, 512877. doi:10.3389/fphar.2020.512877
- GBD 2015 Disease and Injury Incidence and Prevalence Collaborators (2016). Global, Regional, and National Incidence, Prevalence, and Years Lived with Disability for 310 Diseases and Injuries, 1990–2015: a Systematic Analysis for the Global Burden of Disease Study 2015. *Lancet* 388, 1545–1602. doi:10.1016/S0140-6736(16)31678-6
- Gu, L., Lu, J., Li, Q., Wu, N., Zhang, L., Li, H., et al. (2020). A Network-Based Analysis of Key Pharmacological Pathways of Andrographis Paniculata Acting on Alzheimer's Disease and Experimental Validation. *J. Ethnopharmacol* 251, 112488. doi:10.1016/j.jep.2019.112488
- Guo, W., Huang, J., Wang, N., Tan, H. Y., Cheung, F., Chen, F., et al. (2020). Integrating Network Pharmacology and Pharmacological Evaluation for Deciphering the Action Mechanism of Herbal Formula Zuojin Pill in Suppressing Hepatocellular Carcinoma. *Front. Pharmacol.* 10, 1185. doi:10.3389/fphar.2019.01185
- Han, J., Wan, M., Ma, Z., Hu, C., and Yi, H. (2020). Prediction of Targets of Curculigoside A in Osteoporosis and Rheumatoid Arthritis Using Network Pharmacology and Experimental Verification. *Drug Des. Devel Ther.* 14, 5235–5250. doi:10.2147/DDDT.S282112
- Hengartner, M. P., Davies, J., and Read, J. (2019). Antidepressant Withdrawal - the Tide Is Finally Turning. *Epidemiol. Psychiatr. Sci.* 29, e52. doi:10.1017/S2045796019000465

- Jia, J., Liu, M., Wen, Q., He, M., Ouyang, H., Chen, L., et al. (2019). Screening of Anti-complement Active Ingredients from *Eucommia Ulmoides* Oliv. Branches and Their Metabolism *In Vivo* Based on UHPLC-Q-TOF/MS/MS. *J. Chromatogr. B Analyt. Technol. Biomed. Life Sci.* 1124, 26–36. doi:10.1016/j.jchromb.2019.05.029
- Jiang, Y., He, Q., Zhang, T., Xiang, W., Long, Z., and Wu, S. (2020). Exploring the Mechanism of Shengmai Yin for Coronary Heart Disease Based on Systematic Pharmacology and Chemoinformatics. *Biosci. Rep.* 40, BSR20200286. doi:10.1042/BSR20200286
- Khosravi, M., Sotoudeh, G., Amini, M., Raisi, F., Mansoori, A., and Hosseinzadeh, M. (2020). The Relationship between Dietary Patterns and Depression Mediated by Serum Levels of Folate and Vitamin B12. *BMC Psychiatry* 20, 63. doi:10.1186/s12888-020-2455-2
- Kim, J., Lee, S., Choi, B. R., Yang, H., Hwang, Y., Park, J. H., et al. (2017). Sulforaphane Epigenetically Enhances Neuronal BDNF Expression and TrkB Signaling Pathways. *Mol. Nutr. Food Res.* 61, 1–13. doi:10.1002/mnfr.201600194
- Leubner, D., and Hinterberger, T. (2017). Reviewing the Effectiveness of Music Interventions in Treating Depression. *Front. Psychol.* 8, 1109. doi:10.3389/fpsyg.2017.01109
- Levy, M. J. F., Boulle, F., Steinbusch, H. W., van den Hove, D. L. A., Kenis, G., and Lanfumey, L. (2018). Neurotrophic Factors and Neuroplasticity Pathways in the Pathophysiology and Treatment of Depression. *Psychopharmacology (Berl)* 235, 2195–2220. doi:10.1007/s00213-018-4950-4
- Li, L., Zhao, Y., Liu, W., Feng, F., and Xie, N. (2013). HPLC with Quadrupole TOF-MS and Chemometrics Analysis for the Characterization of Folium Turpiniae from Different Regions. *J. Sep. Sci.* 36, 2552–2561. doi:10.1002/jssc.201300360
- Li, X., Qin, X. M., Tian, J. S., Gao, X. X., Du, G. H., and Zhou, Y. Z. (2021). Integrated Network Pharmacology and Metabolomics to Dissect the Combination Mechanisms of Bupleurum Chinense DC-Paeonia Lactiflora Pall Herb Pair for Treating Depression. *J. Ethnopharmacol* 264, 113281. doi:10.1016/j.jep.2020.113281
- Li, Y. F., Huang, Y., Amsdell, S. L., Xiao, L., O'Donnell, J. M., and Zhang, H. T. (2009). Antidepressant- and Anxiolytic-like Effects of the Phosphodiesterase-4 Inhibitor Rolipram on Behavior Depend on Cyclic AMP Response Element Binding Protein-Mediated Neurogenesis in the hippocampus. *Neuropsychopharmacology* 34, 2404–2419. doi:10.1038/npp.2009.66
- Lian, L., Xu, Y., Zhang, J., Yu, Y., Zhu, N., Guan, X., et al. (2018). Antidepressant-like Effects of a Novel Curcumin Derivative J147: Involvement of 5-HT1A Receptor. *Neuropharmacology* 135, 506–513. doi:10.1016/j.neuropharm.2018.04.003
- Liao, M., Song, G., Cheng, X., Diao, X., Sun, Y., and Zhang, L. (2018). Simultaneous Determination of Six Coumarins in Rat Plasma and Metabolites Identification of Bergapten *In Vitro* and *In Vivo*. *J. Agric. Food Chem.* 66, 4602–4613. doi:10.1021/acs.jafc.7b05637
- Liu, M. Y., Yin, C. Y., Zhu, L. J., Zhu, X. H., Xu, C., Luo, C. X., et al. (2018). Sucrose Preference Test for Measurement of Stress-Induced Anhedonia in Mice. *Nat. Protoc.* 13, 1686–1698. doi:10.1038/s41596-018-0011-z
- Liu, Y., Yang, G., and Feng, F. (2016). Integrated Chemical Profiling of Zhi-Zi-Hou-Po Decoction by Liquid Chromatography-Diode Array Detector-Time of Flight Mass Analyzer and Liquid Chromatography-Triple Stage Quadrupole Mass Analyzer Combined with Chemometrics. *Anal. Methods* 8 (23), 4689–4710. doi:10.1039/c6ay01233g
- Luo, K., and Feng, F. (2016). Identification of Absorbed Components and Metabolites of Zhi-Zi-Hou-Po Decoction in Rat Plasma after Oral Administration by an Untargeted Metabolomics-Driven Strategy Based on LC-MS. *Anal. Bioanal. Chem.* 408, 5723–5735. doi:10.1007/s00216-016-9674-x
- Ma, C., Gao, W., Gao, Y., Man, S., Huang, L., and Liu, C. (2011). Identification of Chemical Constituents in Extracts and Rat Plasma from Fructus Aurantii by UPLC-PDA-Q-TOF/MS. *Phytochem. Anal.* 22, 112–118. doi:10.1002/pca.1252
- Nakazawa, T., Yasuda, T., and Ohsawa, K. (2003). Metabolites of Orally Administered Magnolia Officinalis Extract in Rats and Man and its Antidepressant-like Effects in Mice. *J. Pharm. Pharmacol.* 55, 1583–1591. doi:10.1211/0022357022188
- Ou, C., Geng, T., Wang, J., Gao, X., Chen, X., Luo, X., et al. (2020). Systematically Investigating the Pharmacological Mechanism of Dazhu Hongjingtian in the Prevention and Treatment of Acute Mountain Sickness by Integrating UPLC/Q-TOF-MS/MS Analysis and Network Pharmacology. *J. Pharm. Biomed. Anal.* 179, 113028. doi:10.1016/j.jpba.2019.113028
- Ren, L., Tao, W., Zhang, H., Xue, W., Tang, J., Wu, R., et al. (2016). Two Standardized Fractions of Gardenia Jasminoides Ellis with Rapid Antidepressant Effects Are Differentially Associated with BDNF Up-Regulation in the hippocampus. *J. Ethnopharmacol* 187, 66–73. doi:10.1016/j.jep.2016.04.023
- Ren, X., Yu, S., Dong, W., Yin, P., Xu, X., and Zhou, M. (2020). Burden of Depression in China, 1990–2017: Findings from the Global Burden of Disease Study 2017. *J. Affect. Disord.* 268, 95–101. doi:10.1016/j.jad.2020.03.011
- Robson, M. J., Quinlan, M. A., and Blakely, R. D. (2017). Immune System Activation and Depression: Roles of Serotonin in the Central Nervous System and Periphery. *ACS Chem. Neurosci.* 8, 932–942. doi:10.1021/acchemneuro.6b00412
- Ruan, J., Liu, L., Shan, X., Xia, B., and Fu, Q. (2019). Anti-depressant Effects of Oil from Fructus Gardeniae via PKA-CREB-BDNF Signaling. *Biosci. Rep.* 39, BSR20190141. doi:10.1042/BSR20190141
- Shafiee, M., Arekhi, S., Omranzadeh, A., and Sahebkar, A. (2018). Saffron in the Treatment of Depression, Anxiety and Other Mental Disorders: Current Evidence and Potential Mechanisms of Action. *J. Affect. Disord.* 227, 330–337. doi:10.1016/j.jad.2017.11.020
- Shen, Y., Zhang, B., Pang, X., Yang, R., Chen, M., Zhao, J., et al. (2020). Network Pharmacology-Based Analysis of Xiao-Xu-Ming Decoction on the Treatment of Alzheimer's Disease. *Front. Pharmacol.* 11, 595254. doi:10.3389/fphar.2020.595254
- Song, D. K., Suh, H. W., Jung, J. S., Wie, M. B., Son, K. H., and Kim, Y. H. (1996). Antidepressant-like Effects of P-Synephrine in Mouse Models of Immobility Tests. *Neurosci. Lett.* 214, 107–110. doi:10.1016/0304-3940(96)12895-0
- Su, Z., Wang, C., Chang, D., Zhu, X., Sai, C., and Pei, J. (2019). Limonin Attenuates the Stemness of Breast Cancer Cells via Suppressing MIR216A Methylation. *Biomed. Pharmacother.* 112, 108699. doi:10.1016/j.biopha.2019.108699
- Sun, Y., Li, L., Liao, M., Su, M., Wan, C., Zhang, L., et al. (2018). A Systematic Data Acquisition and Mining Strategy for Chemical Profiling of Aster Tataricus Rhizoma (Ziwan) by UHPLC-Q-TOF-MS and the Corresponding Antidepressive Activity Screening. *J. Pharm. Biomed. Anal.* 154, 216–226. doi:10.1016/j.jpba.2018.03.022
- Sun, Y., Zhao, R., Liu, R., Li, T., Ni, S., Wu, H., et al. (2021). Integrated Screening of Effective Anti-insomnia Fractions of Zhi-Zi-Hou-Po Decoction via *Drosophila melanogaster* and Network Pharmacology Analysis of the Underlying Pharmacodynamic Material and Mechanism. *ACS Omega* 6, 9176–9187. doi:10.1021/acsomega.1c00445
- Tang, P., Gu, J. M., Xie, Z. A., Gu, Y., Jie, Z. W., Huang, K. M., et al. (2018). Honokiol Alleviates the Degeneration of Intervertebral Disc via Suppressing the Activation of TXNIP-NLRP3 Inflammasome Signal Pathway. *Free Radic. Biol. Med.* 120, 368–379. doi:10.1016/j.freeradbiomed.2018.04.008
- Tian, Q., and Schwartz, S. J. (2003). Mass Spectrometry and Tandem Mass Spectrometry of Citrus Limonoids. *Anal. Chem.* 75, 5451–5460. doi:10.1021/ac030115w
- Wang, D., Wang, J., Huang, X., Tu, Y., and Ni, K. (2007). Identification of Polymethoxylated Flavones from green Tangerine Peel (*Pericarpium Citri Reticulatae Viride*) by Chromatographic and Spectroscopic Techniques. *J. Pharm. Biomed. Anal.* 44, 63–69. doi:10.1016/j.jpba.2007.01.048
- Wang, J., Zhang, L., Liu, B., Wang, Q., Chen, Y., Wang, Z., et al. (2018). Systematic Investigation of the Erigeron Breviscapus Mechanism for Treating Cerebrovascular Disease. *J. Ethnopharmacol* 224, 429–440. doi:10.1016/j.jep.2018.05.022
- Wang, T., Bai, S., Wang, W., Chen, Z., Chen, J., Liang, Z., et al. (2020). Diterpene Ginkgolides Exert an Antidepressant Effect through the NT3-TrkA and Ras-MAPK Pathways. *Drug Des. Devel. Ther.* 14, 1279–1294. doi:10.2147/DDDT.S229145
- Wang, X. L., Gao, J., Wang, X. Y., Mu, X. F., Wei, S., Xue, L., et al. (2018). Treatment with Shuyu Capsule Increases 5-HT1AR Level and Activation of cAMP-PKA-CREB Pathway in Hippocampal Neurons Treated with Serum from a Rat Model of Depression. *Mol. Med. Rep.* 17, 3575–3582. doi:10.3892/mmr.2017.8339
- Wang, Y., and Feng, F. (2019). Evaluation of the Hepatotoxicity of the Zhi-Zi-Hou-Po Decoction by Combining UPLC-Q-Exactive-MS-Based Metabolomics and

- HPLC-MS/MS-Based Geniposide Tissue Distribution. *Molecules* 24, 511. doi:10.3390/molecules24030511
- Wang, Y., Liu, H., Shen, L., Yao, L., Ma, Y., Yu, D., et al. (2015). Isolation and Purification of Six Iridoid Glycosides from Gardenia Jasminoides Fruit by Medium-Pressure Liquid Chromatography Combined with Macroporous Resin Chromatography. *J. Sep. Sci.* 38, 4119–4126. doi:10.1002/jssc.201500705
- Wang, Y. S., Shen, C. Y., and Jiang, J. G. (2019). Antidepressant Active Ingredients from Herbs and Nutraceuticals Used in TCM: Pharmacological Mechanisms and Prospects for Drug Discovery. *Pharmacol. Res.* 150, 104520. doi:10.1016/j.phrs.2019.104520
- Wu, H., Li, X., Yan, X., An, L., Luo, K., Shao, M., et al. (2015a). An Untargeted Metabolomics-Driven Approach Based on LC-TOF/MS and LC-MS/MS for the Screening of Xenobiotics and Metabolites of Zhi-Zi-Da-Huang Decoction in Rat Plasma. *J. Pharm. Biomed. Anal.* 115, 315–322. doi:10.1016/j.jpba.2015.07.026
- Wu, M., Zhang, H., Zhou, C., Jia, H., Ma, Z., and Zou, Z. (2015b). Identification of the Chemical Constituents in Aqueous Extract of Zhi-Qiao and Evaluation of its Antidepressant Effect. *Molecules* 20, 6925–6940. doi:10.3390/molecules20046925
- Xia, S., Lin, H., Liu, H., Lu, Z., Wang, H., Fan, S., et al. (2019). Honokiol Attenuates Sepsis-Associated Acute Kidney Injury via the Inhibition of Oxidative Stress and Inflammation. *Inflammation* 42, 826–834. doi:10.1007/s10753-018-0937-x
- Xie, Y., Mai, C. T., Zheng, D. C., He, Y. F., Feng, S. L., Li, Y. Z., et al. (2021). Wutou Decoction Ameliorates Experimental Rheumatoid Arthritis via Regulating NF- κ B and Nrf2: Integrating Efficacy-Oriented Compatibility of Traditional Chinese Medicine. *Phytomedicine* 85, 153522. doi:10.1016/j.phymed.2021.153522
- Xing, H., Zhang, K., Zhang, R., Shi, H., Bi, K., and Chen, X. (2015). Antidepressant-like Effect of the Water Extract of the Fixed Combination of Gardenia Jasminoides, Citrus Aurantium and Magnolia Officinalis in a Rat Model of Chronic Unpredictable Mild Stress. *Phytomedicine* 22, 1178–1185. doi:10.1016/j.phymed.2015.09.004
- Xing, H., Zhang, X., Xing, N., Qu, H., and Zhang, K. (2019). Uncovering Pharmacological Mechanisms of Zhi-Zi-Hou-Po Decoction in Chronic Unpredictable Mild Stress Induced Rats through Pharmacokinetics, Monoamine Neurotransmitter and Neurogenesis. *J. Ethnopharmacol.* 243, 112079. doi:10.1016/j.jep.2019.112079
- Xu, W. W., Zheng, C. C., Huang, Y. N., Chen, W. Y., Yang, Q. S., Ren, J. Y., et al. (2018). Synephrine Hydrochloride Suppresses Esophageal Cancer Tumor Growth and Metastatic Potential through Inhibition of Galectin-3-AKT/ERK Signaling. *J. Agric. Food Chem.* 66, 9248–9258. doi:10.1021/acs.jafc.8b04020
- Yao, A. M., Ma, F. F., Zhang, L. L., and Feng, F. (2013). Effect of Aqueous Extract and Fractions of Zhi-Zi-Hou-Pu Decoction against Depression in Inescapable Stressed Mice: Restoration of Monoamine Neurotransmitters in Discrete Brain Regions. *Pharm. Biol.* 51, 213–220. doi:10.3109/13880209.2012.717087
- Ye, J., Cai, S., Cheung, W. M., and Tsang, H. W. H. (2019). An East Meets West Approach to the Understanding of Emotion Dysregulation in Depression: From Perspective to Scientific Evidence. *Front. Psychol.* 10, 574. doi:10.3389/fpsyg.2019.00574
- Yu, G., Wang, W., Wang, X., Xu, M., Zhang, L., Ding, L., et al. (2018). Network Pharmacology-Based Strategy to Investigate Pharmacological Mechanisms of Zuojinwan for Treatment of Gastritis. *BMC Complement. Altern. Med.* 18, 292. doi:10.1186/s12906-018-2356-9
- Yu, S., Liu, H., Li, K., Qin, Z., Qin, X., Zhu, P., et al. (2019). Rapid Characterization of the Absorbed Constituents in Rat Serum after Oral Administration and Action Mechanism of Naozhenneng Granule Using LC-MS and Network Pharmacology. *J. Pharm. Biomed. Anal.* 166, 281–290. doi:10.1016/j.jpba.2019.01.020
- Yu, Y., Wang, J., and Huang, X. (2021). The Anti-depressant Effects of a Novel PDE4 Inhibitor Derived from Resveratrol. *Pharm. Biol.* 59, 418–423. doi:10.1080/13880209.2021.1907422
- Yue, H. L., Zhao, X. H., Wang, Q. L., and Tao, Y. D. (2013). Separation and Purification of Water-Soluble Iridoid Glucosides by High Speed Counter-current Chromatography Combined with Macroporous Resin Column Separation. *J. Chromatogr. B Analyt. Technol. Biomed. Life Sci.* 936, 57–62. doi:10.1016/j.jchromb.2013.08.007
- Zhai, J., Song, Z., Wang, Y., Han, M., Ren, Z., Han, N., et al. (2019). Zhixiong Capsule (ZXC), a Traditional Chinese Patent Medicine, Prevents Atherosclerotic Plaque Formation in Rabbit Carotid Artery and the Related Mechanism Investigation Based on Network Pharmacology and Biological Research. *Phytomedicine* 59, 152776. doi:10.1016/j.phymed.2018.11.036
- Zhang, Q., and Feng, F. (2020). A Novel Insight into the Potential Toxicity Mechanisms of Zhi-Zi-Hou-Po Decoction by Dynamic Urinary Metabolomics Based on UHPLC-Q-Exactive Orbitrap-MS. *J. Chromatogr. B Analyt. Technol. Biomed. Life Sci.* 1142, 122019. doi:10.1016/j.jchromb.2020.122019
- Zhang, R., Zhu, X., Bai, H., and Ning, K. (2019). Network Pharmacology Databases for Traditional Chinese Medicine: Review and Assessment. *Front. Pharmacol.* 10, 123. doi:10.3389/fphar.2019.00123
- Zhang, W., Chen, Y., Jiang, H., Yang, J., Wang, Q., Du, Y., et al. (2020). Integrated Strategy for Accurately Screening Biomarkers Based on Metabolomics Coupled with Network Pharmacology. *Talanta* 211, 120710. doi:10.1016/j.talanta.2020.120710
- Zhang, B., Wang, P. P., Hu, K. L., Li, L. N., Yu, X., Lu, Y., et al. (2019). Antidepressant-Like Effect and Mechanism of Action of Honokiol on the Mouse Lipopolysaccharide (LPS) Depression Model. *Molecules* 24, 2035. doi:10.3390/molecules24112035

Conflict of Interest: The authors declare that the research was conducted in the absence of any commercial or financial relationships that could be construed as a potential conflict of interest.

Publisher's Note: All claims expressed in this article are solely those of the authors and do not necessarily represent those of their affiliated organizations or those of the publisher, the editors, and the reviewers. Any product that may be evaluated in this article or claim that may be made by its manufacturer is not guaranteed or endorsed by the publisher.

Copyright © 2021 Bai, Zhang, Li, Zhang, Wang, He and Ju. This is an open-access article distributed under the terms of the Creative Commons Attribution License (CC BY). The use, distribution or reproduction in other forums is permitted, provided the original author(s) and the copyright owner(s) are credited and that the original publication in this journal is cited, in accordance with accepted academic practice. No use, distribution or reproduction is permitted which does not comply with these terms.